



**HAL**  
open science

# A Turbulent Combustion Model for Jet Flames Issuing in a Vitiated Coflow

Ronan Vicquelin, Benoit Fiorina, Olivier Gicquel

► **To cite this version:**

Ronan Vicquelin, Benoit Fiorina, Olivier Gicquel. A Turbulent Combustion Model for Jet Flames Issuing in a Vitiated Coflow. 23rd International Colloquium on the Dynamics of Explosion and Reactive Systems, Jul 2009, Irvine, United States. hal-01780988

**HAL Id: hal-01780988**

**<https://hal.science/hal-01780988>**

Submitted on 28 Apr 2018

**HAL** is a multi-disciplinary open access archive for the deposit and dissemination of scientific research documents, whether they are published or not. The documents may come from teaching and research institutions in France or abroad, or from public or private research centers.

L'archive ouverte pluridisciplinaire **HAL**, est destinée au dépôt et à la diffusion de documents scientifiques de niveau recherche, publiés ou non, émanant des établissements d'enseignement et de recherche français ou étrangers, des laboratoires publics ou privés.

# A Turbulent Combustion Model for Jet Flames Issuing in a Vitiated Coflow.

Ronan Vicquelin<sup>a</sup>, Benoit Fiorina<sup>b</sup> and Olivier Gicquel<sup>b</sup>

<sup>a</sup>Center for Turbulence Research, Stanford University, Stanford, CA 94305, USA

<sup>b</sup>Ecole Centrale Paris, Laboratoire EM2C, Grande Voie des Vignes,  
92295 Chatenay-Malabry, France

## 1 Introduction

Auto-ignition is of great importance in new technologies like HCCI and MILD combustion where exhaust gases are mixed with fresh gases in order to reduce  $NO_x$  emission while high thermal efficiency is maintained. In many configurations, auto-ignition takes place in a turbulent non-premixed environment [1]. Mathematical modeling becomes very challenging since both chemistry and mixing control the flame.

To facilitate the understanding of auto-ignition in diluted non-premixed flame, the Cabra burner [2, 3] was designed in a simplified configuration: a fuel jet issues in a coflow diluted with burnt gases produced by a secondary burner. The flame studied with hydrogen/nitrogen showed a very high sensitivity of the flame lift-off height in respect to the coflow temperature. Beyond predicting multi-scalar measurements, numerical simulations should also reproduce this lift-off height behavior to validate turbulent combustion models.

Efficiency of transported Probability Density Function (PDF) [2, 4–8] and Conditional Moment Closure (CMC) [9] methods to tackle auto-ignition has been demonstrated in the hydrogen/nitrogen case. Unfortunately, these models remain very expensive in computational resources, especially for industrial applications. Tabulated chemistry models based on flamelets are an alternative strategy which allow considerable CPU saving. This approach was applied to the Cabra methane/air flame [10–12]. However, no tabulated chemistry simulations have reported flame lift-off height sensitivity to the coflow temperature. Here, we develop a turbulent combustion model based on unsteady laminar non-premixed flamelets for RANS simulations. The model, similar to the one used by Ihme and See [12], is applied to the Cabra hydrogen/nitrogen flame whose flame lift-off height is the most sensitive to the coflow temperature in comparison to the methane case. The model, called Unsteady flamelets Tabulated Chemistry (UTaC), is first described. Results are then compared to multi-scalar data and sensitivity analysis to the coflow temperature is conducted.

## 2 The model UTaC

### 2.1 Flamelet equations

Assuming unity species Lewis number (valid even for turbulent hydrogen flames), transient flamelet equations for species mass fractions,  $Y_k$  and temperature,  $T$ , are written as [13]:

$$\rho \frac{\partial Y_k}{\partial \tau} = \frac{\rho \chi}{2} \frac{\partial^2 Y_k}{\partial z^2} + \rho \dot{\omega}_k \quad (1)$$

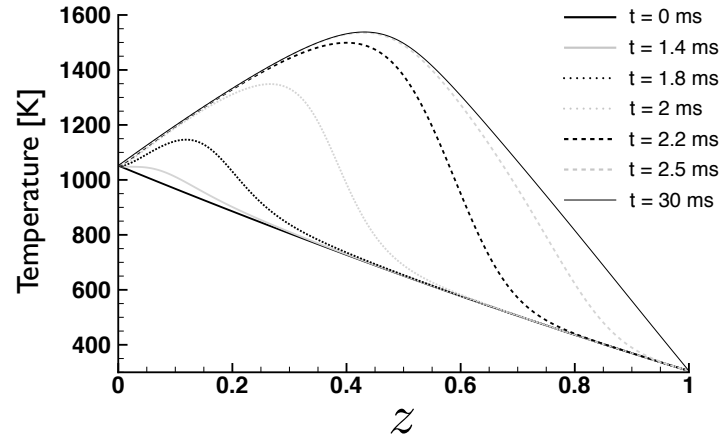


Figure 1: Time evolution of the temperature profile in mixture fraction space. The flamelet was generated with  $\chi_{st}$  fixed to  $100 \text{ s}^{-1}$ .

$$\rho \frac{\partial T}{\partial \tau} = \frac{\rho \chi}{2} \frac{\partial^2 T}{\partial z^2} + \sum_{k=1}^N \frac{\rho h_k \dot{\omega}_k}{c_p} + \frac{\rho \chi}{2} \frac{1}{c_p} \frac{\partial c_p}{\partial z} \frac{\partial T}{\partial z} + \sum_{k=1}^N \frac{\rho \chi}{2} \frac{c_{p_k}}{c_p} \frac{\partial Y_k}{\partial z} \frac{\partial T}{\partial z} \quad (2)$$

$z$ ,  $\rho$ ,  $\dot{\omega}_k$ ,  $h_k$  and  $c_{p_k}$  are respectively the mixture fraction, mass density, the chemical species reaction rates, species enthalpies and species mass heat capacities at constant pressure.  $c_p$  is the mixture heat capacity and  $\lambda$  is the mixture thermal conductivity.  $\chi = 2D_z \left( \frac{\partial z}{\partial x_i} \frac{\partial z}{\partial x_i} \right)$  is the mixture fraction scalar dissipation rate where  $D_z = \frac{\lambda}{\rho c_p}$ . Assuming that the configuration is a counter-flow, the scalar dissipation rate is modeled by [13]:

$$\chi(z) = \chi_{st} \frac{F(z)}{F(z_{st})} \quad (3)$$

where  $F(z) = \frac{1}{\pi} \exp(-2[\text{erf}^{-1}(2z-1)]^2)$  and  $\chi_{st} = \chi(z = z_{st})$  is the stoichiometric scalar dissipation rate. At  $t = 0$ , fuel and oxidizer are mixed, species mass fractions and enthalpy initial profiles are then specified as linear functions of  $z$ . The unsteady flamelet equations are solved with the *FLAMEMASTER* code [14] with a detailed mechanism for hydrogen combustion [15].

Figure 1 shows the evolution of temperature in mixture fraction space for the hydrogen/nitrogen Cabra flame at a given scalar dissipation rate  $\chi_{st} = 100 \text{ s}^{-1}$ . Boundary conditions are given by the reference compositions [2] in fuel and coflow streams except for the coflow temperature which is set to 1052 K instead of 1045 K. Auto-ignition starts preferentially in a lean and hot temperature mixture. The stoichiometric mixture is  $z_{st} = 0.475$  and the most-reactive mixture  $z_{MR}$  is 0.01 where  $z_{MR}$  is the mixture fraction for which the minimal ignition delay is found. Following the early ignition of lean mixtures, a combustion wave propagates in  $z$ -space until the steady solution is reached. Above a critical value  $\chi_{st} = \chi_i$ , auto-ignition does not occur because the flame strain rate is too high.

## 2.2 Turbulent combustion model

A flamelet library composed of unsteady self-igniting flamelets is computed for  $0 < \chi_{st} < \chi_i$  in order to tabulate the chemistry. It captures all the physical phenomena mentioned above. Each flamelet solution is a function of mixture fraction, time and stoichiometric scalar dissipation rate. Any relevant variable can therefore be written as  $\varphi(z, t, \chi_{st})$ . The time variable is substituted by a reaction progress variable,

$c$ , defined as:

$$c = \frac{Y_c(z, t, \chi_{st})}{Y_{c_b}(z, \chi_{st})} \text{ with } Y_c = Y_{H_2O} - Y_{H_2} + Y_{c_0}(z) \quad (4)$$

where  $Y_c$  is the non-normalized progress variable.  $Y_{c_0}(z) = Y_{H_2}(z, t = 0)$  is added to the definition of  $Y_c$  in order to ensure that  $Y_c$  remains positive. In Eq. 4,  $Y_{c_b}$  is introduced for  $c$  to vary between zero and unity for each flamelet solution. Hence,  $Y_{c_b}$  is the steady state burning solution, function of  $z$  and  $\chi_{st}$ . Laminar flamelets quantities are finally tabulated as  $\varphi(z, c, \chi_{st})$ .

In order to use tabulated chemistry in RANS equations, a new chemical table is built by considering presumed Probability Density Functions (PDFs) of input parameters. Assuming independency between  $z$ ,  $c$  and  $\chi_{st}$ , Favre mean quantities are expressed from these parameters PDF,  $P(z^*)$ ,  $P(c^*)$  and  $P(\chi_{st}^*)$ :

$$\tilde{\varphi} = \int_0^{+\infty} \int_0^1 \int_0^1 \varphi(z^*, c^*, \chi_{st}^*) P(z^*) P(c^*) P(\chi_{st}^*) dz^* dc^* d\chi_{st}^* \quad (5)$$

$P(z^*)$  and  $P(c^*)$  are modeled using  $\beta$ -PDF [16] parametrized by the mean and variance of the variables. A log-normal distribution is used to describe the scalar dissipation rate PDF,  $P(\chi_{st}^*)$  with a standard deviation set to 1.0 according to experimental measurements of [17] in turbulent flows. For the integration interval  $[\chi_i, +\infty]$ , unburnt solutions are considered. Averaged thermo-chemical quantities  $\tilde{\phi}$  are computed and stored in a five entries look-up table:  $\tilde{\varphi}(\tilde{z}, z_{var}, \bar{c}, c_{var}, \tilde{\chi}_{st})$ .  $z_{var}$  and  $c_{var}$  are the mixture fraction and progress variable variances. The turbulent combustion model is completed by solving transport equations for  $\tilde{z}$ ,  $z_{var}$ ,  $\tilde{Y}_c$  and  $\tilde{Y}_c^2$ .  $\bar{c}$  and  $c_{var}$  are computed from  $\tilde{Y}_c$  and  $\tilde{Y}_c^2$  [16] and  $\tilde{\chi}_{st}$  is related to the mean scalar dissipation rate:

$$\tilde{\chi}_{st} = \frac{\tilde{\chi}}{\mathcal{F}(\tilde{z}, z_{var})} \text{ with } \mathcal{F}(\tilde{z}, z_{var}) = \int_0^1 \frac{F(z^*)}{F(z_{st})} \tilde{P}(z^*) dz^* \quad (6)$$

$\chi$  is computed from the mean flow field solved with the  $k$ - $\varepsilon$  model:  $\tilde{\chi} = 2D \frac{\partial \tilde{z}}{\partial x_i} \frac{\partial \tilde{z}}{\partial x_i} + 2 \frac{\varepsilon}{k} z_{var}$ .

### 3 Application to the Cabra burner

#### 3.1 Experimental configuration

The Cabra flame was designed to reproduce the stabilization of turbulent flames in a vitiated coflow. In the studied case [2], a 4.57mm-wide round jet injects a hydrogen-nitrogen mixture into a hot coflow of vitiated air. The coflow stream is produced from lean premixed  $H_2$ /air flames. This produces a high temperature mixture composed of air and water vapor. Cabra *et al* [2] specified a coflow temperature of 1045 K, which leads to a flame lifted at  $H/d \approx 10$  ( $d$  is the fuel jet diameter). However,  $H$  is highly sensitive to the coflow temperature [18, 19]: the lift-off height doubles within 20K. As Cabra *et al* reported an experimental uncertainty of 3 % on temperature, the value of 1045 K cannot be trusted to set the numerical simulation. Therefore, the coflow temperature in numerical simulations should be first fitted to find the same lift-off height of 10 diameters before quantitative comparisons [5–7]. In the present work, a coflow temperature of 1052K was chosen to compute the reference  $H_2/N_2$  case. It belongs to the experimental uncertainty range of 3 %.

#### 3.2 Numerical simulation configuration

All RANS simulations are performed with the CFD code CFX [20] on a 2D axisymmetric mesh of 69 000 elements. The number of elements was chosen to ensure grid independence of the solution. A

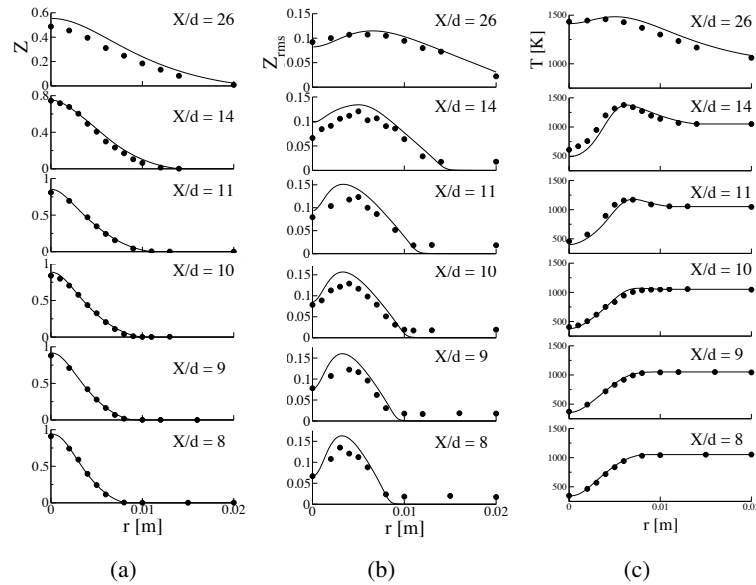


Figure 2: Radial profiles at six axial locations ( $X/d = 8, 9, 10, 11, 14$  and  $26$ ) of Favre mean mixture fraction (a), its RMS (b) and Favre mean temperature (c) of the  $H_2/N_2$  Cabra flame. Line: RANS simulation with the UTaC model. Symbols: experimental data.

known shortcoming of the standard  $k - \varepsilon$  model is its overestimation of the round jet spreading, known as the round jet anomaly. The error can be corrected by changing and specifying ad hoc coefficients in  $k$  and  $\varepsilon$  balance equations. Here, we retain the following set of parameters [21]: all coefficients are fixed by their standard values except for  $C_{\varepsilon 1}$  which is set to 1.6. The turbulent Schmidt number  $Sc_t$  in balance equation for  $\tilde{z}$ ,  $z_{var}$ ,  $\tilde{Y}_c$  and  $\tilde{Y}_c^2$  is fixed to 0.9.

### 3.3 Study of the case $T_{coflow} = 1052$ K

With  $T_{coflow}$  fixed to 1052 K to build the chemical database, the computed flame lift-off height is close to the target value of ten diameters. Numerical results are compared with measurements of Cabra and co-workers [2, 22]. Radial profiles of Favre mean mixture fraction (Fig. 2(a)) and its RMS (Fig. 2(b)) are plotted at six axial locations:  $X/d = 8, 9, 10, 11, 14$  and  $26$ . The very good agreement between numerical and experimental profiles emphasizes the good prediction of mixing between the central jet and the surrounding coflow. Radial profiles of mean temperature are shown in Fig. 2(c). At the first three locations ( $X/d = 8, 9$  and  $10$ ), combustion has not started yet or is not noticeable on temperature profiles. Then, at higher locations ( $X/d = 11, 14$  and  $26$ ), temperature increases first in lean mixtures before ignition spreads to the neighborhood, finishing the transition from fresh to burnt gases. This transition is almost identical in both numerical and experimental profiles.

Favre mean species mass fractions are extracted from the look-up table and compared to experimental radial profiles in Fig. 3. The agreement between numerical and experimental profiles is very good. Even during the ignition phase, intermediate species profiles such as OH are well retrieved, indicating a good representation of the turbulent lifted flame with a library of unsteady non-premixed flamelets. The computed RMS profiles of temperature and species mass fraction also show a good agreement (not shown here).

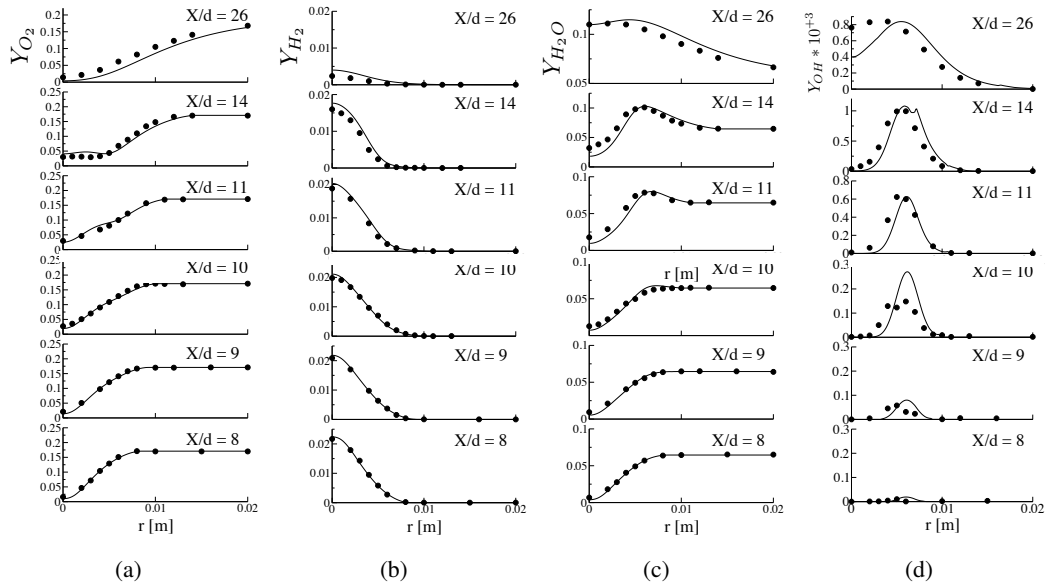


Figure 3: Profiles of Favre mean species mass fractions tabulated in the UTaC database (plain line) and measured (symbols). (a) Radial profiles of  $O_2$ . (b) Radial profiles of  $H_2$ . (c) Radial profiles of  $H_2O$ . (d) Radial profiles of  $OH$ .

### 3.4 Sensitivity to the coflow temperature

Different RANS simulations are performed with five chemical databases that differ by the imposed temperature in the coflow ( $z = 0$ ): 1030 K, 1038 K, 1045 K, 1052 K (used for the reference case) and 1060 K. The resulted lift-off height  $H$  for each simulation is plotted versus the coflow temperature  $T_{cof\text{low}}$  in Fig. 4(a). It is compared to several measured point in the literature [18, 19]. Experimental discrepancies are due to measurement errors on the absolute temperature, however the relative temperature variation is accurate. The numerical profile demonstrates that the computed flame is very sensitive to the coflow temperature:  $H/d$  varies between 8.5 and 28.5 while  $T_{cof\text{low}}$  decreases from 1060 K to 1030 K. Experimental profiles follow the same trend.

In order to facilitate quantitative comparison,  $H$  is plotted in terms of coflow temperature variation  $\Delta T_{cof\text{low}} = T_{cof\text{low}} - T_{ref}$ .  $T_{ref}$  is chosen such as all configurations agree on the same lift-off height when  $\Delta T_{cof\text{low}} = 0$ . The result is given in Fig. 4(b). All curves approximately merge into a single one, even the one computed from the UTaC model. Consequently, the predictive ability of UTaC on the  $H_2/N_2$  is confirmed by the previous quantitative comparisons for  $T_{cof\text{low}} = 1052$  K and by the coflow temperature sensitivity.

## 4 Conclusion

RANS simulations of the hydrogen/nitrogen Cabra flame were performed with the tabulated chemistry model UTaC. By considering unsteady self-igniting flamelets, the model is able to take into account auto-ignition and diffusion flame with a physical transition. Numerical results showed very good agreement with experimental data. The flame lift-off height sensitivity to the coflow temperature, a key feature of this flame, was also retrieved. Such results were previously obtained only with transported PDF or CMC model and demonstrate the efficiency of the UTaC model to predict auto-ignition in non-premixed flames. This work was supported by the ANR-PANH grant of the French Ministry of Research.

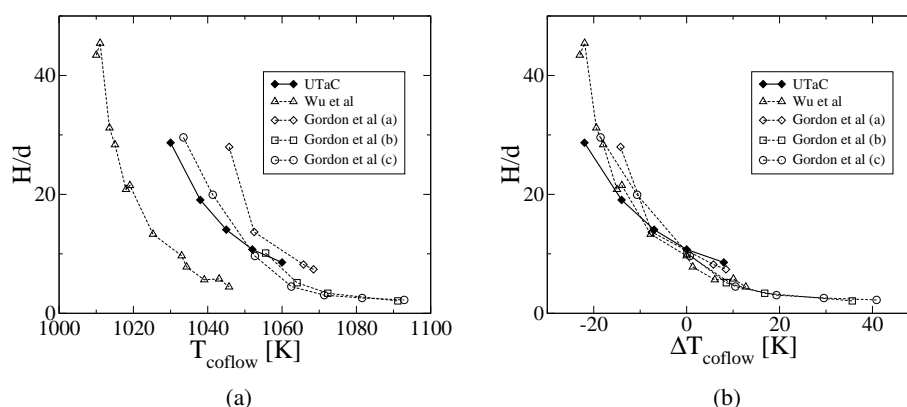


Figure 4: Sensitivity of the lift-off height  $H$  to the coflow temperature ( $d$  is the fuel jet diameter) given by the UTaC model and measurements [18, 19].

## References

- [1] E. Mastorakos. Prog. En. Combust. Sci., 35(1):57–97, 2009.
- [2] R. Cabra, T. Myhrvold, J. Y. Chen, R. W. Dibble, A. N. Karpetis, and R. S. Barlow. Proceedings of the Combustion Institute, 29(2):1881–1888, 2002.
- [3] R. Cabra, J. Y. Chen, R. W. Dibble, A. N. Karpetis, and R. S. Barlow. Combust. Flame, 143(4):491–506, 2005.
- [4] A. R. Masri, R. Cao, S. B. Pope, and G. M. Goldin. Comb. Theory and Modell., 8:1–22, 2004.
- [5] R. Cao, S. B. Pope, and A. R. Masri. Combust. Flame, 142(4):438–453, 2005.
- [6] R. L. Gordon, A. R. Masri, S. B. Pope, and G. M. Goldin. Combust. Theory Modell., 11(3):351–376, 2007.
- [7] W. P. Jones and S. Navarro-Martinez. Combust. Flame, 150(3):170–187, 2007.
- [8] K. Gkagkas and R. P. Lindstedt. Combust. Theory Modell., 13(4):607–643, 2009.
- [9] S. S. Patwardhan, S. De, K. N. Lakshmisha, and B. N. Raghunandan. Proceedings of the Combustion Institute, 32(Part 2):1705–1712, 2009.
- [10] P. Domingo, L. Vervisch, and D. Veynante. Combust. Flame, 152(3):415–432, 2008.
- [11] J.-B. Michel, O. Colin, C. Angelberger, and D. Veynante. Combust. Flame, 156(7):1318 – 1331, 2009.
- [12] M. Ihme and Y. C. See. Combust. Flame, 157(10):1850–1862, 2010.
- [13] N. Peters. Turbulent combustion. Cambridge University Press, 2000.
- [14] H. Pitsch. Technical report, RWTH Aachen, 1998.
- [15] M. Ó Conaire, H. J. Curran, J. M. Simmie, W. J. Pitz, and C. K. Westbrook. Inter. J. Chem. Kin., 36(11):603–622, 2004.
- [16] B. Fiorina, O. Gicquel, L. Vervisch, S. Carpentier, and N. Darabiha. Proceedings of the Combustion Institute, 30:867–874, 2005.
- [17] E. Effelsberg and N. Peters. Proceedings of the Combustion Institute, 22(1):693–700, 1989.
- [18] Z. Wu, S. H. Starner, and R. W. Bilger. Proceedings of the 2003 Australian Symposium on Combustion and the 8th Australian Flame Days, Monash University, Australia, 2003.
- [19] R. L. Gordon, S. H. Starner, A. R. Masri, and R. W. Bilger. Proceedings of the 5th Asia-Pacific Conference on Combustion, pages 333–336, University of Adelaide, Jul 2005.
- [20] ANSYS. Ansys cfx website. <http://www.ansys.com/products/fluid-dynamics/cfx/>, 2010.
- [21] R. L. Gordon, A. R. Masri, S. B. Pope, and G. M. Goldin. Combust. Flame, 151(3):495–511, 2007.
- [22] <http://www.me.berkeley.edu/cal/vcb/index.htm>, 2011.